Rapamycin Pretreatment Rescues the Bone Marrow AML Cell Elimination Capacity of CAR-T Cells

Zhigang Nian[1,2], Xiaohu Zheng[1,2], Yingchao Dou[1,2], Xianghui Du[1,2], Li Zhou[3], Binqing Fu[1,2], Rui Sun[1,2], Zhigang Tian[1,2], and Haiming Wei[1,2]

ABSTRACT

Purpose: Ongoing clinical trials show limited efficacy for Chimeric antigen receptor (CAR) T treatment for acute myeloid leukemia (AML). The aim of this study was to identify potential causes of the reported limited efficacy from CAR-T therapies against AML.

Experimental Design: We generated CAR-T cells targeting Epithelial cell adhesion molecule (EpCAM) and evaluated their killing activity against AML cells. We examined the impacts of modulating mTORC1 and mTORC2 signaling in CAR-T cells in terms of CXCR4 levels. We examined the effects of a rapamycin pretreatment of EpCAM CAR-T cells (during *ex vivo* expansion) and assessed the *in vivo* antitumor efficacy of rapamycin-pretreated EpCAM CAR-T cells (including *CXCR4* knockdown cells) and CD33 CAR-T cells in leukemia xenograft mouse models.

Results: EpCAM CAR-T exhibited killing activity against AML cells but failed to eliminate AML cells in bone marrow. Subse-

quent investigations revealed that aberrantly activated mTORC1 signaling in CAR-T cells results in decreased bone marrow infiltration and decreased the levels of the rapamycin target CXCR4. Attenuating mTORC1 activity with the rapamycin pretreatment increased the capacity of CAR-T cells to infiltrate bone marrow and enhanced the extent of bone marrow AML cell elimination in leukemia xenograft mouse models. *CXCR4* knockdown experiments showed that CXCR4 contributes to the enhanced bone marrow infiltration capacity of EpCAM CAR-T cells and the observed reduction in bone marrow AML cells.

Conclusions: Our study reveals a potential cause for the limited efficacy of CAR-T reported from current AML clinical trials and illustrates an easy-to-implement pretreatment strategy, which enhances the anti-AML efficacy of CAR-T cells.

See related commentary by Maiti and Daver, p. 5739

Introduction

Acute myeloid leukemia (AML) is a hematologic malignancy that develops starting in bone marrow; this is the most common acute leukemia in adults (1, 2). Given that this disease has generally poor outcomes, with 5-year survival rates estimated at 27.4% based on data collected from 2008 to 2014 (3), innovative therapeutics for treating AML are urgently warranted. CD19 chimeric antigen receptor (CAR) T-cell therapy has shown impressive clinical activity against B-cell malignancies (4, 5), and CAR-T cells have been considered a potentially promising immunologic approach for treating AML. Indeed, over the past few years, there have been remarkable achievements (6–10); nevertheless, ongoing clinical

trials are clearly indicating that CAR-T cell-based approaches offer only limited efficacy for treating AML (11, 12).

The clinical trial using Lewis-Y CAR-T cells to treat AML suggests that the therapeutic effects of CAR-T cells are closely associated with CAR-T cell infiltration in the bone marrow (13). Another clinical trial of donor lymphocytes for the treatment of chronic myeloid leukemia (CML) demonstrated that the extent of bone marrow CD8^{+} T-cell infiltration can be used to informatively predict responses to donor lymphocyte infusion in patients with relapsed CML (14). These studies both indicate that the bone marrow migration capacity of CAR-T cells strongly impacts the success of CAR-T cell–based treatments against myeloid leukemia. However, there are now multiple studies showing how *ex vivo* manipulation of CAR-T cells affects the expression of diverse chemokine receptors (15–18) and may change the capacity of CAR-T cells to migrate to bone marrow. Notably, AML cells expressing epithelial cell adhesion molecule (EpCAM) display enhanced tumorigenicity and chemoresistance compared with EpCAM-negative AML cells (19). Given that neither normal bone marrow cells nor PBMCs express EpCAM (19), it is possible that CAR-T targeting EpCAM could represent an effective method for treating AML.

Here, we found that the reduced capacity of EpCAM CAR-T cells to enter bone marrow limited the efficacy of EpCAM CAR-T cell therapeutic activity against AML, and we discovered that *ex vivo* manipulations of EpCAM-targeting CAR-T cells lead to aberrant overactivation of a signaling component that plays a central role in regulating T-cell migration: mTOR (ref. 20). Furthermore, we found that altered mTORC1 signaling causes downregulated expression of CXCR4, a protein known to mediate T-cell migration to bone marrow (21). Applying these basic insights, we found that pharmacologic attenuating mTORC1 activity based on a simple rapamycin pretreatment during *ex vivo* expansion of CAR-T cells upregulated the expression of CXCR4 and found that this pretreatment strongly promoted the migration and penetration capacity of the CAR-T cells

Translational Relevance

Chimeric antigen receptor (CAR)-directed T-cell therapy is a promising immunologic approach for treating acute myeloid leukemia (AML), but the basis of the limited efficacy reported from current clinical trials is not known. Our study revealed that a reduced capacity of CAR-T cells to migrate into bone marrow limits the capacity of the CAR-T cells to eliminate AML cells in bone marrow. Furthermore, we show that a simple pretreatment with rapamycin during *ex vivo* expansion endowed CAR-T cells with a dramatically enhanced capacity to infiltrate bone marrow and promoted AML cell elimination. Our study thus illustrates an approach combining rapamycin and CAR-T cells to treat AML.

for bone marrow, ultimately strongly promoting the elimination capacity against bone marrow–resident AML cells. Finally, experiments with CAR-T cells engineered against a second AML antigen confirmed the ability of our rapamycin-pretreatment strategy to broadly enhance the bone marrow AML cell elimination capacity of CAR-T cells.

Materials and Methods

Mice

Female NOD/ShiLtJGpt-Prkdc[em26Cd52]IL-2rg[em26Cd22]/Gpt (NCG) mice were purchased from GemPharmatech. All mice were kept in specific pathogen-free conditions. All experimental procedures involving mice followed the National Guidelines for Animal Usage in Research (China) and were approved by the Ethics Committee of the University of Science and Technology of China (Hefei, China; Reference No. USTCACUC1701038).

Cell lines

The human myeloid leukemia cell lines (K562, HL60, U937), the human liver cancer cell line (Huh7), the human T-lymphocyte Cell Line (Jurkat), and 293T cell line were purchased from Shanghai Cell Bank (Shanghai, Chinese Academy of Sciences). DNA fingerprinting and isozyme tests were used to identify these cell lines. All cell lines were negative for *Mycoplasma* tested by Mycoplasma Detection Kit (TransGen, FM311). All cell lines were used within 3 months after thawing and detected the *Mycoplasma* every 3 months. K562, HL60, U937, 293T, Huh7, and Jurkat cells were cultured in RPMI1640 (Hyclone) or DMEM (Hyclone) containing 10% FBS (Gibco), 100 U/mL penicillin, 100 μg/mL streptomycin (Solarbio), and 2 mmol/L GlutaMAX (Gibco). K562, HL60, and U937 cells were stably transfected with luciferase. U937-Ep cells were lentivirally transduced with the full-length human *EpCAM* gene as the target cells for the EpCAM CAR-T cells. Primary AML cells from the bone marrow of patients with AML were obtained under the approval of the Ethics Committee of the University of Science and Technology of China (2021-N(H)-120; Hefei, China).

Lentivirus vector construction and production

The EpCAM CAR incorporates the single-chain variable fragment (scFv) derived from the AE4 murine monoclonal hybridoma cell line, a CD8 transmembrane domain, 4–1BB, and the CD3 ζ signaling domains. EpCAM CAR, CD19 CAR (22), or CD33 CAR (9) were inserted into the PCDH-MSCV-MCS-EF1α-copGFP vector (lentiviral transfer vector). The sequence of the short hairpin RNA for CXCR4

was listed in Supplementary Table S1 and was inserted into the pLKO.1-Puro lentiviral transfer vector. Then three kinds of plasmids (lentiviral transfer vector, ps.pAX2 for lentiviral gag-pol, and pMD.2G for VSV-G envelope) were transfected into 293T cells and the supernatants were collected at 48 hours and 72 hours to transduce T cells.

Transduction and expansion of human T cells

Peripheral blood mononuclear cells (PBMC) were separated by density gradient centrifugation, and T cells were separated using a CD3 T-cell Separation Kit (Miltenyi Biotec). On day 0, T cells were resuspended in X-VIVO-15 Medium (Lonza) supplemented with 5% Human AB Serum (GEMINI), 100 U/mL penicillin, 100 μg/mL streptomycin (Solarbio), and 2 mmol/L GlutaMAX (Gibco) at a concentration of 5×10^5 cells/mL, and anti-CD3/CD28 Dynabeads (Thermo Fisher Scientific) were added at a 1: 1 ratio; at the same time, IL2 was added at a final concentration of 100 U/mL and then supplemented every 2 days. After 24 hours, concentrated lentivirus (MOI = 50) and polybrene (Sigma) with a final concentration of 8 μg/mL were added to activated T cells, and were centrifuged at $800 \times g$ for 1 hour at 32°C. The medium was changed after 6–8 hours and rapamycin (Sigma) was added at a final concentration of 20 nmol/L, everolimus (TargetMol, 20 nmol/L), temsirolimus (TargetMol, 20 nmol/L), JR-AB2–011 (TargetMol, 1μmol/L), KU0063794 (TargetMol, 20 nmol/L); Rapamycin was supplemented every 2 days. The cell culture was monitored daily and the medium was added to maintain a cell concentration of $0.5–1 \times 10^6$ cells/mL. On day 4, the Dynabeads were removed. The CAR-T cells were harvested after day 6 for analysis or *in vivo* experiments.

Flow cytometry

The following antibodies were used for flow cytometric analysis: EpCAM-APC (324208, BioLegend), mCD45-PE-CY7 (103114, BioLegend), hCD45-PE (555483, BD), CD45-PerCP-CY5.5 (558714, BD), CXCR4-PE (12–9999–42, eBioscience), p-mTOR Ser2448-PE (583489, BD), p-S6 Ser235/236-APC (14733S, CST), CD3-BV421 (317344, BioLegend), and CD33-PE (555450, BD). Cells isolated from animals or cell lines cultured *in vitro* were washed once in PBS supplemented with 2% FBS (Gibco), and after blocking by Fc receptors, stained at 4°C for 30 minutes in the dark, washed twice with PBS, and then tested. For intracellular staining, cells were first fixed and permeabilized with Foxp3/Transcription Factor Staining Buffer (eBioscience) and then antibody staining was performed. The surface expression of EpCAM CAR was detected by staining with goat anti-mouse $F(ab')^2$ antibody conjugated with Alexa Fluor 647 from Jackson ImmunoResearch. BD LSRII flow cytometry was used for detection, and FlowJo was used for analysis.

Cell killing and cytokine measurements

The *in vitro*–killing activity of EpCAM CAR-T cells, CD33 CAR-T cells, and CD19 CAR-T cells was evaluated by bioluminescence and xCELLigence Real-Time Cell Analyzer (RTCA) Multiple Plate System (ACEA Biosciences).

The bioluminescence method is a luciferase-based assay, as described previously (23). K562, HL60, and U937 cells (10,000 cells/well) stably transduced with luciferase were incubated with EpCAM CAR-T cells, CD33 CAR-T cells, or CD19 CAR-T cells for 16 hours with an indicated effector/target ratios (E:T), the residual luciferase activity of viable tumor cells was measured using a multifunctional microplate reader (CLARIOstar). The cell lysis was calculated as follows: Percentage of lysis = 100-(((average signal from wells treated with T cells)/(average signal from untreated target wells)) × 100).

The xCELLigence Real-Time Cell Analyzer-Multiple Plate system can measure viable adherent target cells in real time. A 50 µL volume of medium was added to each well of the E-Plate 16 (ACEA Biosciences) and the baseline was read, then 100 µL medium containing 10,000 Huh7 cells was added. After the cells were allowed to grow to the logarithmic growth phase, a 50 µL medium containing EpCAM CAR-T cells or untransduced T cells with an indicated effector/target ratios (E:T) was added. The cell index calculated the change in electrical impedance and implies the number of viable target cells. The cell index data in each group were recorded every 15 minutes and showed the average value of the three wells.

The cytokines produced by CAR-T cells *in vitro* were evaluated by incubating CAR-T cells with target cells (100,000 cells/well) at a ratio of 1:1. After 24 hours, the supernatant was collected and the cytokine levels of IL2, TNFα, and IFNγ were measured using ELISA Kits (Dakewe).

qPCR

Control T cells and EpCAM CAR-T cells were collected and resuspended with TRIzol Reagent (Invitrogen). Extracted RNA was reverse transcribed into cDNA with M-MLV Reverse Transcriptase (Thermo Fisher Scientific), and the cDNA was used as the template for qPCR with SYBR Green (Takara). The primers of chemokine receptor are listed in Supplementary Table S2 (three replicates/sample). Relative mRNA expression was calculated by the $\Delta\Delta C_t$ method.

Immunoblotting

Control T cells or CAR-T cells were lysed with RIPA Buffer (Thermo Fisher Scientific) containing 1 mmol/L PMSF(Beyotime) and phosphatase inhibitor cocktail(APE$_X$BIO, 100×), cells were lysed in ice for 30 minutes, then centrifuged at $12,000 \times g$ for 10 minutes and supernatants were collected. After electrophoresis, separated proteins were electroeluted to polyvinylidene difluoride membranes and blocked with 5% w/v milk for 30 minutes at room temperature. Then membranes were incubated with primary antibodies (1:1,000 dilution) overnight at 4°C, then HRP-conjugated antibodies(Sangon) were used for secondary antibodies and enhanced chemiluminescent substrate (Thermo Fisher Scientific) was used for protein level detection.

Antibodies for following proteins were used: PI3K p85 (4257, CST), p-PI3K p85 Tyr458/p55 Tyr199 (4228, CST), Akt (4691, CST), p-Akt Thr308 (13038, CST), p-Akt Ser473 (9271, CST), mTOR (2983, CST), p-mTOR Ser2448 (5536, CST), P70S6K (2708, CST), p-P70S6K Thr389 (9234, CST), 4EBP1(9644, CST), p-4EBP1 Thr37/46 (2855, CST), GAPDH (D110016, Sangon).

Cytokine antibody arrays

Rapamycin-pretreated and nonpretreated EpCAM CAR-T cells were stimulated with HL60 at a ratio of 1:1 for 24 hours at 37°C, 5% CO2, then CAR-T cells were separated using a CD3 T Cell Separation Kit (Miltenyi Biotec).

Cytokine profiles were measured by Human Cytokine Antibody Arrays (Raybiotech, GSH-CAA-440). The operation was according to the manufacturer's instructions. Briefly, (i) sample diluent (100 µL) was added into each well and incubated for 30 minutes to block slides at room temperature; (ii) incubated with 100 µL cell lysates (500 µg/mL) overnight; (iii) Biotinylated Antibody Cocktail was added; (iv) Cy3 Equivalent dye-streptavidin was added and then fluorescence detection was performed; data was analyzed with software GenePix.

Transwell migration assay

Migration was measured by 5 µm pore 24 well Transwell Plates (Costar). The lower chamber was added 500 µL of RPMI1640 complete medium containing 100 ng/mL CXCL12 (absin), and then the upper chamber was filled with 200 µL RPMI1640 complete medium containing control T cells or EpCAM CAR-T cells or rapamycin-treated EpCAM CAR-T cells (1×10^5). Plates were incubated for 4 hours at 37°C and 5% CO$_2$, then all cells in the lower chamber were collected and centrifuged at $300 \times g$ for 5 minutes at 4°C, Resuspended in culture medium, and counted using a hemocytometer.

IHC staining

The mouse tibia or femur tissue was fixed in 4% paraformaldehyde solution overnight and embedded after decalcification, and 4 µm bone sections were obtained for IHC staining, anti-human EpCAM antibody (ab223582, Abcam, 1:500 dilution) or anti-human CD33 antibody(ab269456, Abcam, 1:200 dilution) was used to label AML cells, and anti-human CD45 antibody (#13917, CST, 1:200 dilution) or anti-human CD3 antibody (#85061, CST, 1:200 dilution) was used to label human T cells in the mouse bone marrow. Images were taken by Mshot microscope (MF50) and analyzed by MShot Image Analysis System (software).

RNA sequencing

Control T cells and EpCAM CAR-T cells were cultured *in vitro* for 6 days and then collected and resuspended with TRIzol Reagent (Invitrogen). Samples were library prepped and sequenced via Illumina NextSeq. $n = 3$ human donors. RNA-seq data were deposited into the National Center for Biotechnology Information Gene Expression Omnibus repository (accession number: GSE162796).

Corrected *P* value of 0.05 and absolute fold change of 2 were set as the threshold for significantly differential expression.

Xenograft mouse models

HL60 labeled with luciferase, U937-Ep cells, or primary AML cells from the bone marrow of patients with AML were transferred to female NCG mice (6–10 weeks) by tail vein or tibia injection to establish a leukemia xenograft model, tumor formation was determined on day 5–6, and then CAR-T cells were transferred via the tail vein. AML burden was monitored by bioluminescence imaging using the IVIS Spectrum Imaging System (Perkin Elmer) or detected by flow cytometer at the indicated time points. Quantitative image data were analyzed using Living Image Software (Perkin Elmer).

Statistical analysis

Prism 6.0 (GraphPad version 6) was used to determine statistical significance. Two-tailed unpaired or paired Student *t* test between the two groups and one-way ANOVA between multiple groups were used to determine significance. A log-rank test was used to test for differences in overall survival. The data represent the mean ± SD; $P < 0.05$ is considered significant (*, $P < 0.05$; **, $P < 0.01$; ***, $P < 0.005$; ****, $P < 0.0001$).

Results

EpCAM CAR-T cells fail to eliminate bone marrow leukemia cells

We previously reported that EpCAM overexpression in AML cells and EpCAM$^+$ AML cells resulted in enhanced tumorigenicity and chemoresistance (19), indicating that EpCAM is a potential therapeutic target for AML. Therefore, we generated CAR-T cells targeting human EpCAM incorporating EpCAM single-chain variable fragment (scFv), which was derived from the AE4 murine monoclonal hybridoma cell line, the CD8 transmembrane domain, 41BB costimulatory domain, and CD3ζ signal transduction domain (24). CD19 CAR was
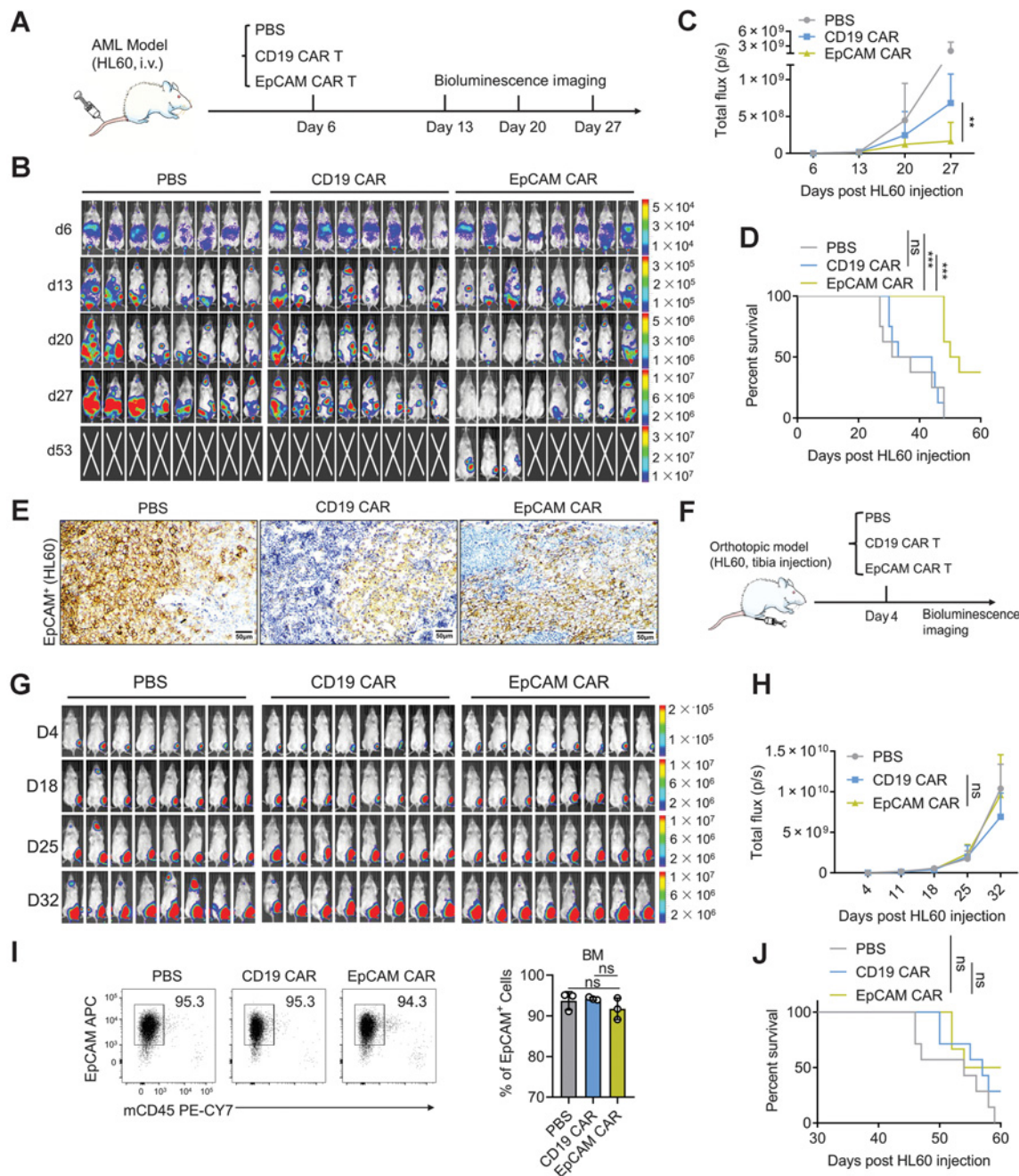
Figure 1.

EpCAM CAR-T cells have difficulty clearing bone marrow AML cells. **A,** Experimental scheme: NCG mice were injected with 5×10^6 HL60 cells stably expressing luciferase into the tail vein, followed by transfer of PBS, 5×10^6 CD19 CAR-T cells, or 5×10^6 EpCAM CAR-T cells for treatment; AML burdens were monitored by bioluminescence imaging once each week for 3 weeks. $n = 8$ mice per group. The experiment was performed twice. **B,** Bioluminescence imaging of AML burdens. **C,** AML burdens were quantified as the average values of the total radiance (photons; data shown as mean ± SD; unpaired, two-tailed Student t test). **D,** Kaplan–Meier survival analysis. $n = 8$ mice per group. Statistical significance was determined by log-rank Mantel–Cox test (median survival, PBS group: 34 days, CD19 CAR-T cells group: 38.5 days, EpCAM CAR-T cells group: 51.5 days). **E,** IHC staining of the bone marrow (tibia) with an anti-human EpCAM antibody to label EpCAM$^+$ tumor cells (HL60) in the PBS-treated group, CD19 CAR-T cells group, and EpCAM CAR-T cells group. Error bars, 50 μm. **F,** Experimental scheme: NCG mice were injected 1×10^5 HL60 cells stably expressing luciferase into the tibia, followed by transfer of PBS, 4×10^6 CD19 CAR-T cells, or 4×10^6 EpCAM CAR-T cells (via the tail vein). AML burdens were monitored by bioluminescence imaging once each week for 4 weeks. $n = 8$ mice per group. The experiment was performed twice. **G,** Bioluminescence imaging of AML burdens. **H,** AML burdens were quantified as average values of the total radiance (photons; data shown as mean ± SD; unpaired, two-tailed Student t test). **I,** Representative flow cytometry plot of the proportion of EpCAM$^+$ mCD45$^-$ AML cells (HL60) in the bone marrow (tibia) of the PBS group, CD19 CAR-T cells group, and EpCAM CAR-T cells group. $n = 3$ mice per group (data shown as mean ± SD ordinary one-way ANOVA with Tukey multiple comparisons test). **J,** Kaplan–Meier survival analysis, statistical significance was determined by log-rank Mantel–Cox test. (median survival, PBS group: 54 days, CD19 CAR group: 57 days, EpCAM CAR group: 57 days; *, $P < 0.05$; **, $P < 0.01$; ***, $P < 0.001$; ****, $P < 0.0001$. ns, not significant).
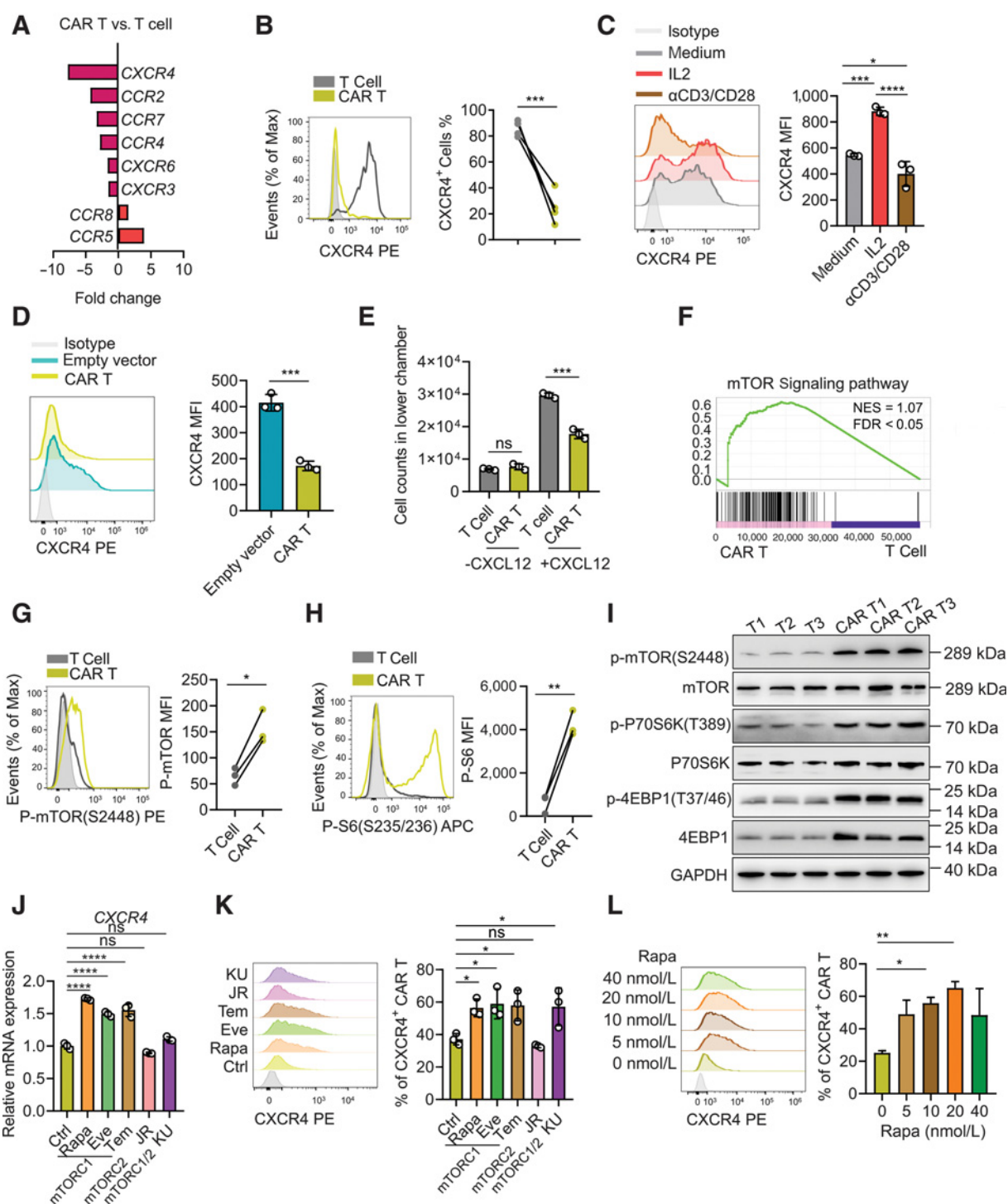
Figure 2.
Activation of mTORC1 signaling decreases the CXCR4 level in EpCAM CAR-T cells. **A,** Fold-changes in transcription level of chemokine receptor genes in EpCAM CAR-T cell compared with control T cells, $n = 3$ human donors. **B,** FACS analysis of the proportion of CXCR4$^+$ cells in control T cells and CAR-T cells. $n = 4$ normal human donors. Paired two-tailed Student t test. **C,** FACS analysis of CXCR4 expression in control T cells, T cells cultured with IL2 (100 U/mL), T cells stimulated with CD3/CD28 antibody (data shown as mean ± SD; one-way ANOVA with Tukey multiple comparisons test). **D,** FACS analysis of CXCR4 expression in T cells modified with control empty vector and EpCAM CAR-T cells. (data shown as mean ± SD; unpaired two-tailed Student t test). **E,** Transwell analysis of the counts of the control T cells (unmodified T cells) and EpCAM CAR-T cells that migrated to the lower chamber in response to CXCL12 (100 ng/mL). "-CXCL12," without CXCL12 in the lower chamber; "+CXCL12," with CXCL12 in the lower chamber (data shown as mean ± SD; unpaired two-tailed Student t test). Data shown are representative of three independent experiments.   (*Continued on the following page.*)

used as a negative control (Supplementary Fig. S1A; ref. 22). To initially characterize the efficacy of the CAR construct, we first transduced the CAR into Jurkat cells and observed that the transduction efficiency was more than 90% (Supplementary Fig. S1B). Colabeling with an anti-mouse Fab antibody and green fluorescent protein confirmed the expression of CAR on the membrane surface (Supplementary Fig. S1C). Next, we used EpCAM[+] Huh7 liver cancer cells as target cells and found that CAR Jurkat cells could effectively kill the EpCAM^{+} Huh7 cells, whereas untransduced (control) Jurkat cells had almost no killing activity (Supplementary Fig. S1D), establishing that the CAR structure is effective in promoting cytotoxicity.

Next, we transduced our EpCAM CAR construct into primary human T cells, which achieved 76.2% transduction efficiency (Supplementary Fig. S1E), and then incubated the CAR-T cells with the EpCAM[+] myeloid leukemia cell lines K562 and HL60 for 16 hours (Supplementary Fig. S1F). The EpCAM CAR-T cells, but not CD19 CAR-T cells, mediated potent lysis of EpCAM[+] K562 and HL60 cells (Supplementary Fig. S1G and S1H). We also incubated EpCAM CAR-T cells or CD19 CAR-T cells with target K562 and HL60 cells (1:1 cell ratio) for 24 hours and then collected the supernatant to analyze cytokine levels. Although the samples with EpCAM CAR-T cells produced high levels of IFNγ, TNFα, and IL2, these cytokines were barely detected in the CD19 CAR-T cell group (Supplementary Fig. S1I and S1J). These results together demonstrate that our EpCAM CAR-T cells have strong killing activity against EpCAM^{+} cells.

To evaluate the therapeutic activity of EpCAM CAR-T cells *in vivo*, we injected luciferase-labeled HL60 cells into NCG (NOD/ShiLtJGpt-Prkdc[em26Cd52]IL-2rg[em26Cd22]/Gpt) mice (tail vein injection) to induce a leukemia xenograft model (**Fig. 1A**; ref. 19). Compared with the PBS-treated control group and the CD19 CAR-T cell treatment control group, the EpCAM CAR-T cell–treated-group had reduced AML burdens throughout the early stages of treatment (day 6–27); however, we observed that 4/8 mice in the EpCAM CAR-T cell–treated-group still had obvious AML lesions on day 27, with especially evident lesions in bone marrow (**Fig. 1B** and **C**). Although our data showed that the EpCAM CAR-T cell–treated did prolong mouse survival times (**Fig. 1D**), our bioluminescence imaging clearly indicated that the EpCAM CAR-T cells had failed to control tumor growth in bone marrow as assessed in the later stage of treatment (day 53; **Fig. 1B**), Indeed, IHC analyses revealed many EpCAM^{+} tumor cells in bone marrow samples examined from postmortem mice of the EpCAM CAR-T cell treatment group (**Fig. 1E**). These findings suggest that EpCAM CAR-T cells may be unable to effectively eliminate AML cells in bone marrow.

To further investigate the capacity of CAR-T cells to eliminate bone marrow AML cells, we established a bone marrow orthotopic xenograft model by injecting luciferase-labeled HL60 cells into mouse tibia, after confirmation of engraftment by bioluminescence imaging, mice

were treated with PBS, CD19 CAR-T cells, or EpCAM CAR-T cells by tail vein injection. (**Fig. 1F**). There were no significant differences in AML burden in the PBS-, CD19 CAR-T cell-, or EpCAM CAR-T cell–treated groups (**Fig. 1G** and **H**), indicating that EpCAM CAR-T cells could not effectively remove AML cells from bone marrow. Flow cytometry analysis showed that mCD45^{−}EpCAM^{+} human AML cells had completely occupied the bone marrow of mice all of the three experimental groups (**Fig. 1I**), and EpCAM CAR-T cell treatment did not extend mouse survival times (**Fig. 1J**). These data clearly indicate that CAR-T cells cannot effectively eliminate AML cells resident in bone marrow.

Activation of mTORC1 signaling decreases the CXCR4 level and reduces the bone marrow migration capacity of EpCAM CAR-T cells

To explore potential causes for the observed inability of CAR-T cells to eliminate bone marrow AML cells, we analyzed the transcriptomes of control T cells and EpCAM CAR-T cells during *ex vivo* expansion. KEGG analysis showed significantly differential expression of genes involved in chemokine signaling between control T cells and EpCAM CAR-T cells (Corrected *P* value of 0.05 and absolute fold change of 2; Supplementary Fig. S2A). Next, we compared the transcription level of chemokine receptors and found that *CXCR4*, a chemokine receptor that is known to mediate T-cell migration to bone marrow (21), was significantly downregulated in EpCAM CAR-T cells compared with control T cells (**Fig. 2A**). Further supporting this, flow cytometry analysis indicated that the surface CXCR4 expression on EpCAM CAR-T cells was only 24.78% versus 85.73% for control T cells (**Fig. 2B**).

Although there are various CAR designs and distinctive scFv targeting tumor antigens, the manufacturing procedures for CAR-T are consistent, involving: (i) isolation, (ii) activation, and (iii) genetic modification. CD3/CD28 antibodies are widely used for T-cell activation, and IL2 is a common cytokine used in CAR-T cell culture (25). We next tested factors that may affect CXCR4 expression during *ex vivo* manipulation of CAR-T cells. We first added IL2 to the isolated T cells and found that IL2 upregulated the expression of CXCR4. However, stimulating T cells with anti-CD3/CD28 antibodies significantly downregulated the expression of CXCR4 compared with control T cells (**Fig. 2C**). Furthermore, we found that the expression of CXCR4 in EpCAM CAR-T cells was significantly lower than in T cells modified with the control empty vector (**Fig. 2D**), indicating that CAR signaling apparently somehow downregulates CXCR4 expression.

CXCL12 is the ligand of CXCR4 (26) and is secreted by bone marrow stromal cells (27); CXCL12 mediates the migration of immune cells into bone marrow (28). We used Transwell assays to evaluate the migration of control T cells and EpCAM CAR-T cells in response to CXCL12. Without CXCL12 in the lower chamber, the number of cells that migrated to the lower chamber did not differ between EpCAM

(*Continued.*) **F,** GSEA suggesting that EpCAM CAR-T cells are significantly enriched for the expression of transcripts with functional annotations related to the mTOR signaling pathway compared with control T cells (Enrichment plot: mTOR signaling pathway). **G** and **H,** FACS analysis of the phosphorylation of mTOR (**G**) and ribosomal protein S6 (**H**) in EpCAM CAR-T cells and control T cells, $n = 3$ normal human donors, paired two-tailed Student t test. **I,** Immunoblot analysis of mTOR signaling components in control T cells and EpCAM CAR-T cells, $n = 3$ normal human donors. Data are representative of two experiments. **J,** Transcription level of *CXCR4* in EpCAM CAR-T cells treated with DMSO, rapamycin, everolimus, temsirolimus, JR-AB2–011, and KU0063794 for 24 hours, $n = 3$ (data shown as mean ± SD ordinary one-way ANOVA with Tukey multiple comparison test). **K,** FACS analysis of the proportion of CXCR4^{+} EpCAM CAR-T cells treated with DMSO, rapamycin, everolimus, temsirolimus, JR-AB2–011, and KU0063794 for 24 hours, $n = 3$ (data shown as mean ± SD; ordinary one-way ANOVA with Tukey multiple comparison test). **L,** FACS analysis of the proportion of CXCR4^{+} EpCAM CAR-T cells treated with 0 nmol/L, 5 nmol/L, 10 nmol/L, 20 nmol/L, and 40 nmol/L rapamycin for 6 days. ($n = 3$, data shown as mean + SD; unpaired two-tailed Student t test; *, $P < 0.05$; **, $P < 0.01$; ***, $P < 0.001$; ****, $P < 0.0001$, ns, not significant).
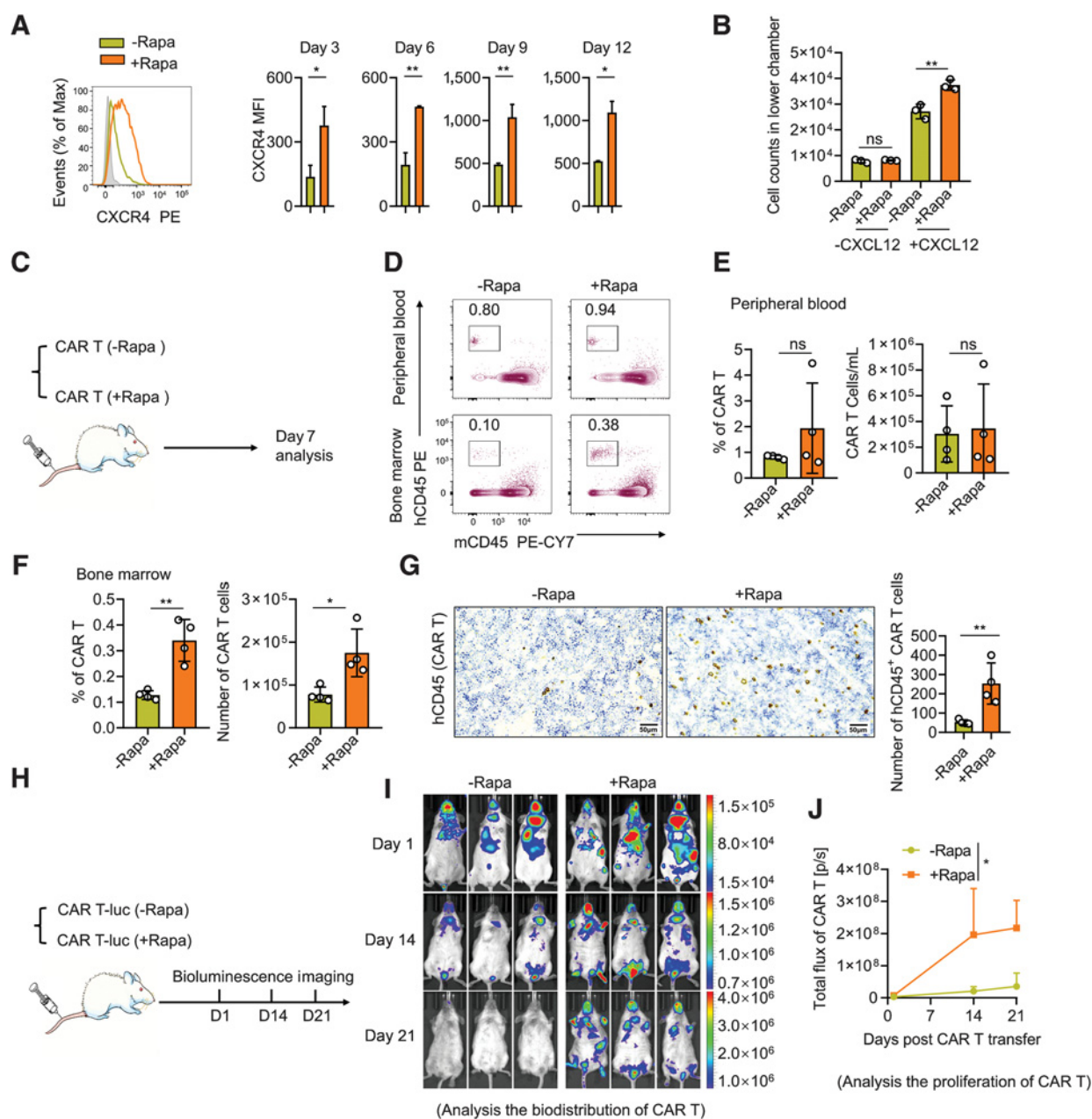
Figure 3.
Rapamycin pretreatment promotes EpCAM CAR-T cells bone marrow migration by upregulating the expression of CXCR4. **A,** FACS analysis of CXCR4 expression of rapamycin-pretreated CAR-T cells or nonpretreated CAR-T cells at different culture time points. $n = 3$ human donors (data shown as mean ± SD; unpaired two-tailed Student t test). **B,** Transwell analysis of the counts of rapamycin-pretreated EpCAM CAR-T cells and nonpretreated EpCAM CAR-T cells that migrated to the lower chamber in response to CXCL12 (100 ng/mL). "-CXCL12," without CXCL12 in the lower chamber; "+CXCL12," with CXCL12 in the lower chamber (data shown as mean ± SD; unpaired two-tailed Student t test). Data shown are representative of three independent experiments. **C,** Experimental scheme: NCG mice were transferred 5 × 10^6 rapamycin-pretreated EpCAM CAR-T cells or nonpretreated EpCAM CAR-T cells into the tail vein, 7 days after transfer, the mice were euthanized and were analyzed by flow cytometry. $n = 4$ mice per group. The experiment was performed twice. **D,** FACS analysis of the proportion of hCD45$^+$mCD45$^-$ EpCAM CAR-T cells in the peripheral blood and bone marrow (tibia). **E** and **F,** The proportion and quantity of rapamycin-pretreated EpCAM CAR-T cells or nonpretreated CAR-T cells in the peripheral blood (**E**) and bone marrow (**F**). $n = 4$ mice per group (data shown as mean ± SD; unpaired two-tailed Student t test). **G,** IHC staining of bone marrow (tibia) with an anti-human CD45 antibody to label hCD45$^+$ CAR-T cells in the rapamycin-pretreated group and nonpretreated group (left). Error bars, 50 μm. The number of hCD45$^+$ CAR-T cells in the bone marrow sections (right). $n = 4$ mice per group, data shown as mean ± SD, unpaired two-tailed Student t test. **H,** Experimental scheme: NCG mice were transferred with 5 × 10^6 rapamycin-pretreated and nonpretreated EpCAM CAR-T cells, both labeled with luciferase, into the tail vein, the biodistribution and proliferation of CAR-T cells *in vivo* was monitored by bioluminescence imaging at the indicated times. $n = 3$ mice per group. The experiment was performed twice. **I,** Image of the biodistribution of CAR-T cells by bioluminescence imaging. **J,** Proliferation of CAR-T cells was quantified as the average values of the total radiance (photons). $n = 3$ mice per group (data shown as mean ± SD; unpaired two-tailed Student t test; *, $P < 0.05$; **, $P < 0.01$; ***, $P < 0.001$; ****, $P < 0.0001$, ns, not significant).
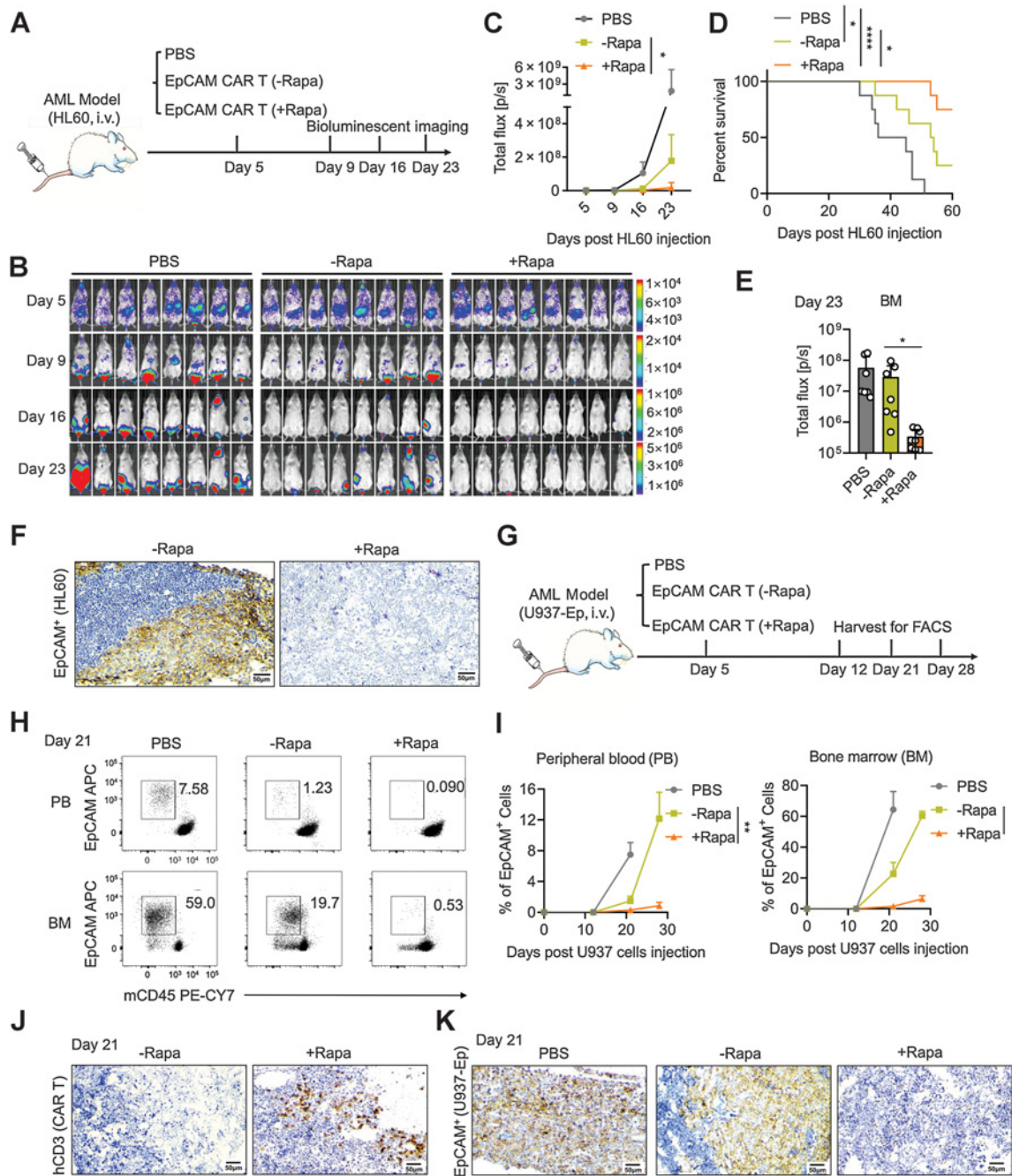
Figure 4.
Rapamycin pretreatment enhances the bone marrow AML cells elimination capacity of EpCAM CAR-T cells. **A,** Experimental scheme: NCG mice were injected with 1×10^6 HL60 stably expressing luciferase into the tail vein, then transferred PBS, 1×10^6 rapamycin-pretreated EpCAM CAR-T cells or nonpretreated EpCAM CAR-T cells, and AML burdens were monitored by bioluminescence once each week for 3 weeks. $n = 8$ mice per group. The experiment was performed twice. **B,** Bioluminescence imaging of AML burdens. **C,** AML burdens in the whole body were quantified as the average values of the total radiance (photons; data shown as mean ± SD; unpaired, two-tailed Student t test). **D,** Kaplan–Meier survival analysis. $n = 8$ mice per group. Statistical significance was determined by the log-rank Mantel–Cox test. (median survival, PBS group: 40.5 days, rapamycin nonpretreated group: 53.5 days, rapamycin-pretreated group: undefined). **E,** AML burdens in the bone marrow area (femur and tibia, one side) on day 23 were quantified as the total radiance (photons; data shown as mean ± SD; unpaired, two-tailed Student t test). **F,** IHC staining of bone marrow (tibia) with an anti-human EpCAM antibody to label EpCAM$^+$ tumor cells (HL60) in the rapamycin-pretreated group and nonpretreated group, Error bars, 50 μm. **G,** Experimental scheme: NCG mice were injected with 1×10^6 U937 stably expressing EpCAM into the tail vein, then transferred PBS, 1×10^6 rapamycin-pretreated EpCAM CAR-T cells or nonpretreated EpCAM CAR-T cells, and AML burdens in the peripheral blood and bone marrow (femur and tibia) were detected by flow cytometry once each week for 3 weeks. $n = 9$ mice per group. The experiment was performed twice. **H,** Representative flow cytometry plot of the proportion of EpCAM$^+$ mCD45$^-$ AML cells in the peripheral blood and bone marrow on day 21. **I,** AML burden shown as the proportion of EpCAM$^+$ mCD45$^-$ AML cells in the peripheral blood and bone marrow, all mice in the PBS group were dead within 28 days. (data shown as mean ± SD; unpaired, two-tailed Student t test). **J,** IHC staining of bone marrow (tibia) with an anti-human CD3 antibody to label CD3$^+$ CAR-T cells in the rapamycin-pretreated and nonpretreated group. Error bars, 50 μm. **K,** IHC staining of bone marrow (tibia) with an anti-human EpCAM antibody to label EpCAM$^+$ tumor cells (U937-Ep) on day 21 in the PBS group, the rapamycin-pretreated group, and nonpretreated group, Error bars, 50 μm (*, $P < 0.05$; **, $P < 0.01$; ***, $P < 0.001$; ****, $P < 0.0001$).
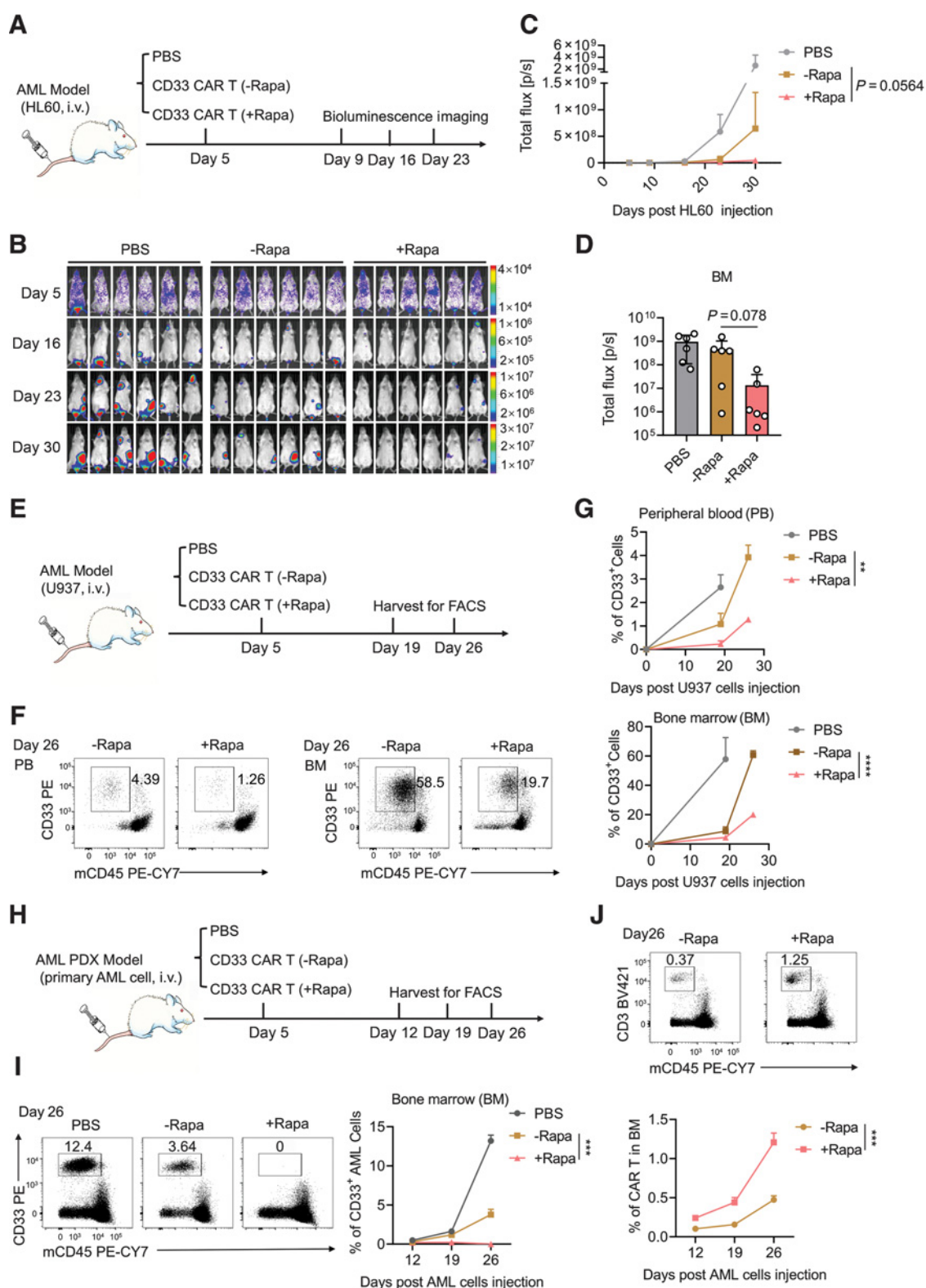
Figure 5.
Rapamycin pretreatment of CD33 CAR-T cells enhances the extent of bone marrow AML cell elimination. **A,** Experimental scheme: NCG mice were injected 1×10^6 HL60 stably expressing luciferase into the tail vein, then transferred PBS, 1×10^6 rapamycin-pretreated CD33 CAR-T cells or nonpretreated CD33 CAR-T cells, and AML burdens were monitored by bioluminescence imaging once each week for 4 weeks. $n = 6$ mice per group. (*Continued on the following page.*)

CAR-T cells and control T cells. In contrast, with CXCL12 in the lower chamber, the number of EpCAM CAR-T cells that migrated to the lower chamber was significantly reduced compared with control T cells (**Fig. 2E**); results indicate that CAR T cells have a reduced capacity to respond to CXCL12 and suggest that the reduced bone marrow migration capacity is a potential cause for the failure to eliminate bone marrow AML cells of EpCAM CAR-T cells.

Next, we explored potential causes of the observed reduction in CXCR4 levels, specifically by assessing the transcriptional profiles of control T cells and EpCAM CAR-T cells. KEGG analysis showed enrichment for genes involved in the PI3K-Akt signaling pathways among the control T cells and EpCAM CAR-T cell differentially expressed genes (Corrected *P* value of 0.05 and absolute fold change of 2; Supplementary Fig. S2A). However, our analysis of PI3K-Akt signaling components from the RNA-seq dataset indicated upregulation of the levels of mTOR-related genes (the downstream of PI3K-Akt) but not PI3K-Akt–related genes *per se* (Supplementary Fig. S2B). Furthermore, a GSEA analysis suggested that the mTOR signaling pathway was significantly activated in the EpCAM CAR-T cells (**Fig. 2F**), and previous studies have reported that attenuation of mTOR activity was accompanied by increased CXCR4 expression (29).

Pursuing this, we examined the phosphorylation of PI3K and Akt in control T cell and EpCAM CAR-T cells: there is no difference between the two sample types (Supplementary Fig. S2C). We also examined the phosphorylation of mTOR signaling components: this revealed elevation of the p-mTOR, P70S6K, S6, and 4EBP1 levels in the EpCAM CAR-T cells (**Fig. 2G–I**).

We selectively blocked different mTOR signaling complexes by using mTORC1 inhibitors (rapamycin, everolimus, temsirolimus; refs. 30–32), an mTORC2 inhibitor (JR-AB2–011; ref. 33), or an mTORC1/2 dual inhibitor (KU0063794; Supplementary Fig. S2D; ref. 34). The CXCR4 level in EpCAM CAR-T cells was significantly increased upon treatment with mTORC1 inhibitors and the dual inhibitor but not upon treatment with the mTORC2 inhibitor (**Fig. 2J** and **K**). These results indicate that activation of mTORC1 signaling reduces CXCR4 levels.

Rapamycin is a classic inhibitor of mTORC1 kinase, which has been approved as a treatment to prevent rejection of transplanted organs (31). Optimization testing showed that a 20 nmol/L rapamycin pretreatment induced the greatest extent of CXCR4 expression in EpCAM CAR-T cells (**Fig. 2L**). Furthermore, cytokine antibody arrays showed that rapamycin pretreatment did not affect the cytokine profile of EpCAM CAR-T cells (Supplementary Fig. S3A; ref. 35). Moreover, *in vitro*–killing assays showed that rapamycin pretreatment did not alter the killing activity of EpCAM CAR-T cells for AML cells (Supplementary Fig. S3B).

Attenuating mTORC1 activity with rapamycin promotes EpCAM CAR-T cell bone marrow migration by upregulating CXCR4

To explore whether rapamycin pretreatment can promote the migration of EpCAM CAR-T cells to bone marrow, we first assessed the CXCR4 expression of rapamycin-pretreated or nonpretreated EpCAM CAR-T cells during *ex vivo* expansion (day 3, 6, 9, 12) and found that rapamycin pretreatment both significantly upregulated CXCR4 expression in EpCAM CAR-T cells (**Fig. 3A**). Furthermore, we also evaluated the ability of EpCAM CAR-T cells in response to CXCL12 by Transwell. Without CXCL12 in the lower chamber, the number of cells that migrated to the lower chamber had no difference between rapamycin-pretreated CAR-T cells and nonpretreated CAR-T cells, whereas with CXCL12 in the lower chamber, the number of rapamycin-pretreated CAR-T cells that migrated to the lower chamber was significantly more than nonpretreated CAR-T cells (**Fig. 3B**), which indicates that rapamycin-pretreated CAR-T cells have an increased capacity to repose to CXCL12 and suggests that rapamycin pretreatment may promote EpCAM CAR-T cells to migrate to bone marrow.

Pursuing this idea, we transferred rapamycin-pretreated or nonpretreated EpCAM CAR-T cells into NCG mice. All mice were euthanized 7 days after transfer, and the peripheral blood and bone marrow were collected for analysis (**Fig. 3C**). We found that rapamycin pretreatment did not impact the distribution of EpCAM CAR-T cells in the peripheral blood (**Fig. 3D** and **E**); however, rapamycin pretreatment significantly increased the quantity and percentage of EpCAM CAR-T cells that migrated to bone marrow (**Fig. 3D** and **F**). IHC staining also showed that the number of CAR-T cells infiltration in the bone marrow of the rapamycin-pretreated group was significantly more than the nonpretreated group (**Fig. 3G**), indicating that rapamycin pretreatment promotes EpCAM CAR-T cells bone marrow migration.

To exclude the influence of individual differences of mice, we labeled rapamycin-pretreated EpCAM CAR-T cells with CellTrace Violet, then 1:1 mixed with nonpretreated EpCAM CAR-T cells and transferred into NCG mice. The peripheral blood and bone marrow were collected 7 days after transfer as well (Supplementary Fig. S4A). We also found that rapamycin pretreatment did not impact the distribution of EpCAM CAR-T cells in peripheral blood; however, the percentage of CellTrace Violet$^+$ rapamycin-pretreated CAR-T cells in bone marrow was significantly higher than nonpretreated CAR-T cells (Supplementary Fig. S4B and S4C).

To validate whether rapamycin-pretreated CAR-T cells can long-term exist in bone marrow, we transferred rapamycin-pretreated or nonpretreated EpCAM CAR-T cells, both labeled with luciferase, into NCG mice (**Fig. 3H**), and monitored the biodistribution of CAR-T cells using bioluminescence imaging. As was seen in bioluminescence

---

(*Continued.*) The experiment was performed twice. **B,** Bioluminescence imaging of AML burdens. **C,** AML burdens in the whole body was quantified as average values of the total radiance (photons). $n = 6$ mice per group. (data shown as mean ± SD; unpaired, two-tailed Student *t* test). **D,** AML burdens in the bone marrow area (femur and tibia, one side) on day 30 were quantified as the total radiance (photons). $n = 6$ mice per group. (data shown as mean ± SD; unpaired, two-tailed Student *t* test). **E,** Experimental scheme: NCG mice were injected with 1×10^6 U937 into the tail vein, then transferred PBS, 1×10^6 rapamycin-pretreated CD33 CAR-T cells or nonpretreated CD33 CAR-T cells. AML burdens in the peripheral blood and bone marrow (femur and tibia) were detected by flow cytometry. $n = 6$ mice per group. The experiment was performed twice. **F,** Representative flow cytometry plot of the proportion of CD33$^+$ mCD45$^-$ AML cells in the peripheral blood and bone marrow on day 26. **G,** AML burdens shown as the proportion of CD33$^+$ mCD45$^-$ AML cells in the peripheral blood and bone marrow, all mice in the PBS group were dead within 26 days (data shown as mean ± SD; unpaired, two-tailed Student *t* test). **H,** Experimental scheme: NCG mice were injected with 1×10^7 primary AML cells into the tail vein to establish the AML PDX model; mice were then treated with PBS, 1×10^6 rapamycin-pretreated CD33 CAR-T cells, or nonpretreated CD33 CAR-T cells. AML burdens and CAR-T cell infiltration into bone marrow (femur and tibia) were detected by flow cytometry. $n = 9$ mice per group. The experiment was performed twice. **I,** FACS analysis of the proportion of CD33$^+$ mCD45$^-$ AML cells in the bone marrow (data shown as the mean ± SD; unpaired, two-tailed Student *t* test). **J,** FACS analysis of the proportion of CD3$^+$ mCD45$^-$ CAR-T cells in the bone marrow (data shown as the mean ± SD; unpaired, two-tailed Student *t* test; *, $P < 0.05$; **, $P < 0.01$; ***, $P < 0.001$; ****, $P < 0.0001$, ns, not significant).

image, nonpretreated EpCAM CAR-T cells hardly migrate to bone marrow, in contrast, rapamycin-pretreated EpCAM CAR-T cells effectively migrate to bone marrow and long-term–existed in bone marrow (**Fig. 3I**). Furthermore, when we extend the time point of peripheral blood sample collection to 14 days after transfer, we found that the percentage and quantity of CAR-T cells in the rapamycin-pretreated group was significantly higher than the nonpretreated group (Supplementary Fig. S5A). The changes in total radiance reflected the proliferation of CAR-T cells. Compared with nonpretreated CAR-T cells, rapamycin-pretreated CAR-T cells had a stronger proliferation (**Fig. 3J**). These data indicate that rapamycin pretreatment increases migration of CAR-T cells to the bone marrow and prolongs survival of CAR-T cells.

Overall, our study illustrates an easy-to-implement strategy to promote EpCAM CAR-T cells to migrate to bone marrow and the enhanced bone marrow migration capacity may promote EpCAM CAR-T cell to eliminate bone marrow AML cells.

Rapamycin pretreatment promotes EpCAM CAR-T cell to eliminate bone marrow AML cells

To validate whether rapamycin-pretreated CAR-T cells have an enhanced capacity to eliminate bone marrow AML cells, we compared rapamycin-pretreated EpCAM CAR-T cells and nonpretreated EpCAM CAR-T cells in an *in vivo* model. To more closely model the clinical situation of leukemia, we established a leukemia xenograft model based on injecting luciferase-labeled HL60 cells into NCG mice by tail vein instead of tibia. After confirmation of engraftment by bioluminescence imaging, mice were transferred with rapamycin-pretreated EpCAM CAR-T cells (pretreated with 20 nmol/L rapamycin for 6 days) or nonpretreated EpCAM CAR-T cells, and the AML burden was monitored using bioluminescence imaging (**Fig. 4A**). Peripheral blood samples were taken and serum was prepared 2 days after the transfer of CAR-T cells. No differences in IFNγ levels were detected between rapamycin-pretreated versus nonpretreated EpCAM CAR-T cells (Supplementary Fig. S6A), indicating that rapamycin pretreatment does not affect the killing activity of CAR-T cells *in vivo*. Compared with nonpretreated CAR-T cells group, rapamycin-pretreated CAR-T cells resulted in a significantly lower AML burden and longer survival time of mice (**Fig. 4B–D**).

Next, we calculated the total radiance in bone marrow area of mice, which reflected AML burden in bone marrow. The rapamycin-pretreated group was significantly lower than the nonpretreated group (**Fig. 4E**). IHC analyses showed that EpCAM$^+$ AML cells were not observed in bone marrow of rapamycin-pretreated group 60 days after HL60 injection, whereas many infiltrated AML cells were present in bone marrow of the nonpretreated group (**Fig. 4F**). These data suggest that rapamycin-pretreated EpCAM CAR-T cells have an enhanced capacity to eliminate bone marrow AML cells.

To confirm that rapamycin-pretreated EpCAM CAR-T cells have an enhanced capacity to eliminate bone marrow AML cells, we used another AML cell line, U937-Ep cells (U937 cells were overexpressed with human EpCAM full-length gene by lentiviral; Supplementary Fig. S6B), to construct a leukemia xenograft model, and AML residues (mCD45$^-$EpCAM$^+$ cells) after treatment of EpCAM CAR-T cells in the peripheral blood and bone marrow were monitored by flow cytometry (**Fig. 4G**). Similar AML residues were observed in the peripheral blood between rapamycin-pretreated group and nonpretreated group on day 21; however, contrary to many AML cells resided in bone marrow of nonpretreated group, no AML cells were detected in rapamycin-pretreated group (**Fig. 4H**). Finally, rapamycin-pretreated

group had significantly lower AML residues than nonpretreated group both in peripheral blood and bone marrow (**Fig. 4I**). IHC analyses from sacrificed mice on day 21 showed similar results: the rapamycin-pretreated group had CAR-T cell infiltration in bone marrow and no EpCAM$^+$ AML cells, whereas many EpCAM$^+$ AML cells were observed in bone marrow of PBS-treated group and nonpretreated group (**Fig. 4J** and **K**). These data demonstrate that rapamycin-pretreated EpCAM CAR-T cells exerted enhanced anti-bone marrow AML capacity.

Moreover, we used lentiviruses expressing shCXCR4 to knock down CXCR4 in rapamycin-pretreated EpCAM CAR-T cells (Supplementary Fig. S7A and S7B) and observed reduced migration of these cells into bone marrow (Supplementary Fig. S7C and S7D). The extent of bone marrow AML cell elimination was also reduced in the mice given the CXCR4 knockdown rapamycin-pretreated EpCAM CAR-T cells (Supplementary Fig. S7E).

Rapamycin pretreatment enhances anti-bone marrow AML capacity of CD33 CAR-T cells

To investigate whether rapamycin treatment is also applicable to CAR-T cells engineered against other AML target proteins, like CD33, a promising target for AML therapies (9, 36), which is also expressed in HL60 cells (Supplementary Fig. S8A). After confirming that CD33 CAR-T cells had increased CXCR4 level upon treatment with rapamycin and effectively killed CD33$^+$ HL60 cells *in vitro* (Supplementary Fig. S8B and S8C), luciferase-labeled HL60 cells were injected into NCG mice via the tail vein to establish a leukemia xenograft model, and mice were treated via transfer of rapamycin-pretreated CD33 CAR-T cells or nonpretreated CD33 CAR-T cells (**Fig. 5A**). The results of CD33 CAR-T cells were similar to EpCAM CAR-T cells. Compared with nonpretreated CD33 CAR-T cells, rapamycin-pretreated CD33 CAR-T cells resulted in a significantly lower AML burden (**Fig. 5B** and **C**). Next, we also calculated the total radiance in bone marrow area of mice. The rapamycin-pretreated group was significantly lower than the nonpretreated group (**Fig. 5D**).

Another AML cell line, U937 cells, also expressed CD33 (Supplementary Fig. S8D). To confirm that rapamycin-pretreated CD33 CAR-T cells has an enhanced capacity to eliminate bone marrow AML cells, U937 cells were injected into NCG mice (via tail vein) to establish a leukemia xenograft model as previous, followed by transfer of rapamycin-pretreated CD33 CAR-T cells or nonpretreated CD33 CAR-T cells (**Fig. 5E**). Similarly, rapamycin-pretreated group had significantly lower AML residues than nonpretreated group both in the peripheral blood and bone marrow (**Fig. 5F** and **G**).

Primary AML cells have a greater extent of clonal heterogeneity than established AML cell lines and are thus considered to be relatively more informative materials for experiments related to human disease (9). We collected CD33$^+$ bone marrow cells from patients with AML and injected those cells into NCG mice (via tail vein) to establish an AML patient-derived xenograft (PDX) model (Supplementary Fig. S8E; **Fig. 5H**). As with our initial findings in the cell line xenograft model, we found that the rapamycin-pretreated group had significantly lower AML residues and more CAR-T cell infiltration in the bone marrow than the nonpretreated group (**Fig. 5I** and **J**). IHC analyses also showed a similar result (Supplementary Fig. S8F).

These results with CAR-T cells engineered to target antigens other than EpCAM support that our rapamycin pretreatment strategy apparently broadly enhances the bone marrow AML cell elimination capacity of CAR-T cells.

Discussion

AML is a disease with a high recurrence rate and low 5-year survival rates (1), so innovative approaches for AML therapies are needed. CAR-T cells are a potential therapeutic approach for AML, but it is clear that obtaining therapeutic benefits will require that CAR-T cells can migrate into bone marrow to access (and eliminate) AML cells. Our study reveals a potential cause for the limited efficacy of CAR-T in the AML treatment: CAR-T cells downregulate the expression of CXCR4 during *ex vivo* expansion, which results in a decreased *in vivo* capacity for migrating to bone marrow, thereby substantially weakening the ability of the CAR-T cells to eliminate bone marrow AML cells. Stimulating T cells with anti-CD3/CD28 antibodies and tonic CAR signaling both strengthen the activation of the mTOR signaling (37, 38), which causes downregulation of CXCR4. We found that attenuating mTORC1 activation with rapamycin can overcome this artifact of *ex vivo* CAR-T cell manipulation, promoting CXCR4 accumulation and thereby increasing the bone marrow migration capacity of CAR-T cells. Ultimately, the rapamycin-pretreated CAR-T cells have an enhanced therapeutic efficacy against AML.

The persistence of CAR-T cells has been associated with both initial efficacy and sustained remission effects (39, 40), and previous studies have reported that pretreatment with various inhibitors during *ex vivo* manipulation can both modulate T-cell terminal differentiation and improve *in vivo* persistence (37, 41). Obviously, CAR-T cells must be able to migrate to the tumor site to enable therapeutic efficacy. Previous studies have shown that modulating the migration capacity of CAR-T cells can be achieved on the basis of overexpression of chemokine receptors through genetic modification (15, 17, 18). However, our study clearly shows that an easy strategy—inhibitor pretreatment—is also suitable for modulating the bone marrow migration capacity of CAR-T cells. Extrapolating from this, it seems plausible that this pretreatment strategy may also help solve additional migration-related problems limiting the success of adoptive cell therapies.

We show that rapamycin pretreatment can enhance the capacity of both EpCAM CAR-T cells and CD33 CAR-T cells to eliminate bone marrow AML cells, indicating that our strategy is not limited to a single target, that is, this pretreatment strategy is apparently suitable for improving the bone marrow AML elimination capacity of CAR-T cells engineered to target a variety of AML antigens. It also bears strong emphasis that the simplicity of *in vitro* rapamycin pretreatment should make this strategy easy to generalize to the manufacture of CAR-T cells for AML treatment. Thus, our study has clear clinical implications, and it should be remembered that rapamycin has been approved for clinical use in transplantation indications (31). Overall, our study illustrates an easy-to-implement strategy that strongly enhances the bone marrow leukemia cell elimination capacity of CAR-T cells and provides a basis for a planned clinical trial using rapamycin-pretreated CAR-T cell against AML.

References

1. Döhner H, Weisdorf DJ, Bloomfield CD. Acute myeloid leukemia. N Engl J Med 2015;373:1136–52.
2. Perna F, Berman SH, Soni RK, Mansilla-Soto J, Eyquem J, Hamieh M, et al. Integrating proteomics and transcriptomics for systematic combinatorial chimeric antigen receptor therapy of AML. Cancer Cell 2017;32: 506–19.
3. Hofmann S, Schubert M-L, Wang L, He B, Neuber B, Dreger P, et al. Chimeric antigen receptor (CAR) T cell therapy in acute myeloid leukemia (AML). J Clin Med 2019;8:200.
4. June CH, Sadelain M. Chimeric antigen receptor therapy. N Engl J Med 2018;379: 64–73.
5. Maude SL, Frey N, Shaw PA, Aplenc R, Barrett DM, Bunin NJ, et al. Chimeric antigen receptor T cells for sustained remissions in leukemia. N Engl J Med 2014; 371:1507–17.
6. Gill S, Tasian SK, Ruella M, Shestova O, Li Y, Porter DL, et al. Preclinical targeting of human acute myeloid leukemia and myeloablation using chimeric antigen receptor-modified T cells. Blood 2014;123:2343–54.
7. Mardiros A, Dos SC, McDonald T, Brown CE, Wang X, Budde LE, et al. T cells expressing CD123-specific chimeric antigen receptors exhibit specific cytolytic effector functions and antitumor effects against human acute myeloid leukemia. Blood 2013;122:3138–48.
8. Lynn RC, Poussin M, Kalota A, Feng Y, Low PS, Dimitrov DS, et al. Targeting of folate receptor β on acute myeloid leukemia blasts with chimeric antigen receptor-expressing T cells. Blood 2015;125:3466–76.
9. Kenderian SS, Ruella M, Shestova O, Klichinsky M, Aikawa V, Morrissette JJ, et al. CD33-specific chimeric antigen receptor T cells exhibit potent preclinical activity against human acute myeloid leukemia. Leukemia 2015;29:1637–47.
10. Casucci M, Nicolis di Robilant B, Falcone L, Camisa B, Norelli M, Genovese P, et al. CD44v6-targeted T cells mediate potent antitumor effects against acute myeloid leukemia and multiple myeloma. Blood 2013;122:3461–72.
11. Fan M, Li M, Gao L, Geng S, Wang J, Wang Y, et al. Chimeric antigen receptors for adoptive T cell therapy in acute myeloid leukemia. J Hematol Oncol 2017;10: 151.
12. Mardiana S, Gill S. CAR T cells for acute myeloid leukemia: state of the art and future directions. Front Oncol 2020;10:697.
13. Ritchie DS, Neeson PJ, Khot A, Peinert S, Tai T, Tainton K, et al. Persistence and efficacy of second generation CAR T cell against the ley antigen in acute myeloid leukemia. Mol Ther 2013;21:2122–9.
14. Bachireddy P, Hainz U, Rooney M, Pozdnyakova O, Aldridge J, Zhang W, et al. Reversal of in situ T-cell exhaustion during effective human antileukemia responses to donor lymphocyte infusion. Blood 2014;123:1412–21.
15. Di Stasi A, De Angelis B, Rooney CM, Zhang L, Mahendravada A, Foster AE, et al. T lymphocytes coexpressing CCR4 and a chimeric antigen receptor targeting CD30 have improved homing and antitumor activity in a Hodgkin tumor model. Blood 2009;113:6392–402.
16. Liu G, Rui W, Zheng H, Huang D, Yu F, Zhang Y, et al. CXCR2-modified CAR-T cells have enhanced trafficking ability that improves treatment of hepatocellular carcinoma. Eur J Immunol 2020;50:712–24.

17. Craddock JA, Lu A, Bear A, Pule M, Brenner MK, Rooney CM, et al. Enhanced tumor trafficking of GD2 chimeric antigen receptor T cells by expression of the chemokine receptor CCR2b. J Immunother 2010;33:780–8.

18. Moon EK, Carpenito C, Sun J, Wang LCS, Kapoor V, Predina J, et al. Expression of a functional CCR2 receptor enhances tumor localization and tumor eradication by retargeted human t cells expressing a mesothelin-specific chimeric antibody receptor. Clin Cancer Res 2011;17:4719–30.

19. Zheng X, Fan X, Fu B, Zheng M, Zhang A, Zhong K, et al. EpCAM inhibition sensitizes chemoresistant leukemia to immune surveillance. Cancer Res 2017;77: 482–93.

20. Chi H. Regulation and function of mTOR signalling in T cell fate decisions. Nat Rev Immunol 2012;12:325–38.

21. Arojo OA, Ouyang X, Liu D, Meng T, Kaech SM, Pereira JP, et al. Active mTORC2 signaling in naive T cells suppresses bone marrow homing by inhibiting CXCR4 expression. J Immunol 2018;201:908–15.

22. Imai C, Mihara K, Andreansky M, Nicholson IC, Pui CH, Geiger TL, et al. Chimeric receptors with 4–1BB signaling capacity provoke potent cytotoxicity against acute lymphoblastic leukemia. Leukemia 2004;18:676–84.

23. Mount CW, Majzner RG, Sundaresh S, Arnold EP, Kadapakkam M, Haile S, et al. Potent antitumor efficacy of anti-GD2 CAR T cells in H3-K27M+ diffuse midline gliomas. Nat Med 2018;24:572–9.

24. Long AH, Haso WM, Shern JF, Wanhainen KM, Murgai M, Ingaramo M, et al. 4–1BB costimulation ameliorates T cell exhaustion induced by tonic signaling of chimeric antigen receptors. Nat Med 2015;21:581–90.

25. Wang X, Rivière I. Clinical manufacturing of CAR T cells: foundation of a promising therapy. Mol Ther Oncolytics 2016;3:16015.

26. Janssens R, Struyf S, Proost P. The unique structural and functional features of CXCL12. Cell Mol Immunol 2018;15:299–311.

27. Zhao E, Xu H, Wang L, Kryczek I, Wu K, Hu Y, et al. Bone marrow and the control of immunity. Cell Mol Immunol 2012;9:11–9.

28. Bleul CC, Fuhlbrigge RC, Casasnovas JM, Aiuti A, Springer TA. A highly efficacious lymphocyte chemoattractant, stromal cell-derived factor 1 (SDF-1). J Exp Med 1996;184:1101–9.

29. Collins N, Han SJ, Enamorado M, Link VM, Huang B, Moseman EA, et al. The bone marrow protects and optimizes immunological memory during dietary restriction. Cell 2019;178:1088–101.

30. Lane HA, Wood JM, McSheehy PM, Allegrini PR, Boulay A, Brueggen J, et al. mTOR inhibitor RAD001 (everolimus) has antiangiogenic/vascular properties distinct from a VEGFR tyrosine kinase inhibitor. Clin Cancer Res 2009;15: 1612–22.

31. Chueh SCJ, Kahan BD. Clinical application of sirolimus in renal transplantation: an update. Transpl Int 2005;18:261–77.

32. Shor B, Zhang WG, Toral-Barza L, Lucas J, Abraham RT, Gibbons JJ, et al. A new pharmacologic action of CCI-779 involves FKBP12-independent inhibition of mTOR kinase activity and profound repression of global protein synthesis. Cancer Res 2008;68:2934–43.

33. Benavides-Serrato A, Lee J, Holmes B, Landon KA, Bashir T, Jung ME, et al. Correction: specific blockade of Rictor-mTOR association inhibits mTORC2 activity and is cytotoxic in glioblastoma. PLoS One 2019;14: e0212160.

34. García-Martínez JM, Moran J, Clarke RG, Gray A, Cosulich SC, Chresta CM, et al. Ku-0063794 is a specific inhibitor of the mammalian target of rapamycin (mTOR). Biochem J 2009;421:29–42.

35. Rossi J, Paczkowski P, Shen Y-W, Morse K, Flynn B, Kaiser A, et al. Preinfusion polyfunctional anti-CD19 chimeric antigen receptor T cells are associated with clinical outcomes in NHL. Blood 2018;132:804–14.

36. Kim MY, Yu KR, Kenderian SS, Ruella M, Chen S, Shin TH, et al. Genetic inactivation of CD33 in hematopoietic stem cells to enable CAR T cell immunotherapy for acute myeloid leukemia. Cell 2018;173: 1439–53.

37. Zheng W, O'Hear CE, Alli R, Basham JH, Abdelsamed HA, Palmer LE, et al. PI3K orchestration of the in vivo persistence of chimeric antigen receptor-modified T cells. Leukemia 2018;32:1157–67.

38. Scholz G, Jandus C, Zhang L, Grandclément C, Lopez-Mejia IC, Soneson C, et al. Modulation of mTOR signalling triggers the formation of stem cell-like memory T cells. EBioMedicine 2016;4:50–61.

39. Brentjens RJ, Rivière I, Park JH, Davila ML, Wang X, Stefanski J, et al. Safety and persistence of adoptively transferred autologous CD19-targeted T cells in patients with relapsed or chemotherapy refractory B-cell leukemias. Blood 2011;118:4817–28.

40. Grupp SA, Kalos M, Barrett D, Aplenc R, Porter DL, Rheingold SR, et al. Chimeric antigen receptor-modified T cells for acute lymphoid leukemia. N Engl J Med 2013;368:1509–18.

41. Kagoya Y, Nakatsugawa M, Yamashita Y, Ochi T, Guo T, Anczurowski M, et al. BET bromodomain inhibition enhances T cell persistence and function in adoptive immunotherapy models. J Clin Invest 2016;126:3479–94.